36

Semiconductor few-electron quantum dots as spin qubits

J. M. ELZERMAN, R. HANSON, L. H. WILLEMS VAN BEVEREN,
L. M. K. VANDERSYPEN, AND L. P. KOUWENHOVEN

Kavli Institute of Nanoscience Delft and ERATO Mesoscopic Correlation Project, Delft University of Technology, PO Box 5046, 2600 GA Delft, The Netherlands

Abstract

The experimental steps taken towards using the spin of a single electron trapped in a semiconductor quantum dot as a spin qubit[1] is described. Fabrication and characterization of a double quantum dot containing two coupled spins has been achieved, as well as initialization and single-shot read-out of the spin state. The single-spin relaxation time was found to be of the order of a millisecond, but the decoherence time is still unknown. Concrete ideas – using a charge detection approach – on how to proceed towards demonstrating superposition and entanglement of spin states are presented. Single-spin manipulation relies on a microfabricated wire located close to the quantum dot, and two-spin interactions are controlled via the tunnel barrier connecting the respective quantum dots.

36.1 Qubit

Any implementation of a quantum bit has to satisfy the five DiVincenzo requirements.[2] The first requirement is to have a scalable physical system with well-characterized qubits. Double quantum dot devices have been fabricated in which a single electron can be confined in each of the two dots.[3] The spin states $\uparrow$ and $\downarrow$ of the electron, subject to a large magnetic field B, correspond to the two states of the proposed qubit twolevel system. The Zeeman splitting, ΔE_Z, between the two states can be tuned with the magnetic field, according to $\Delta E_Z = g\mu_B B$, with $g \approx -0.44$ the electron g-factor in GaAs,[4] and μ_B the Bohr magneton.

These one-electron dots can be fully characterized using a QPC as a charge detector.[3,4] First of all, the QPC can be used to monitor the charge configuration of the double dot, in order to reach the regime where both dots contain just a single electron. Then the tunnel rate from each dot to the reservoir can be evaluated and tuned using a lock-in technique. The same technique can be employed to determine the energy spectrum of each of the two dots, i.e., the Zeeman splitting between the two qubit states, as well as the energy of orbital excited states. Furthermore, the QPC can be used to monitor the inter-dot tunnel barrier, both qualitatively (from the

curvature of lines in the honeycomb diagram) and quantitatively (by performing photon-assisted tunneling spectroscopy to measure the tunnel splitting between the one-electron bonding and antibonding state[5]). In principle, it is even possible to use the lock-in technique to measure the exchange splitting J between the delocalized two-electron singlet and triplet spin states. However, in practical situations the splitting might be too small ($< 20\,\mu$eV) to be resolved using tunneling spectroscopy.

All relevant parameters of the two-spin system can thus be determined without performing transport measurements. The essential advantage of the QPC technique is that it works even for a dot that is very weakly coupled to just a *single* reservoir, with a tunnel rate between zero and ~ 100 kHz (limited by the bandwidth of the current measurement setup). This gives us more freedom to design simpler dots with fewer gates, which could therefore be easier to operate.

36.2 Read-out

Single-shot read-out of the spin orientation of an individual electron in a quantum dot[6] has been achieved. The approach used here utilizes the Zeeman splitting, induced by a large magnetic field parallel to the 2DEG, to create spin-to-charge conversion (Fig. 36.1a). This is followed by real-time detection of single-electron tunneling events using the QPC. The total visibility of the spin measurement is $\sim 65\%$, limited mostly by the ~ 40 kHz bandwidth of our current measurement setup, and also by thermal excitation of electrons out of the quantum dot, due to the high effective electron temperature of ~ 300 mK.

It was estimated that the visibility of the spin read-out technique could be improved to more than 90% by lowering the electron temperature below 100 mK, and especially by using a faster way to measure the charge on the dot. This could be possible with a 'Radio-Frequency QPC' (RF-QPC), similar to the well-known RF-SET.[7] In this approach, the QPC is embedded in an LC circuit with a resonant frequency of ~ 1 GHz. By measuring the reflection or transmission of a resonant carrier wave, it is estimated that it should be possible to read out the charge state of the nearby quantum dot in $\sim 1\,\mu$s, an order of magnitude faster than is currently attainable.

A disadvantage of the read-out technique based on the Zeeman splitting is that it relies on accurate positioning of the dot-levels with respect to the Fermi energy of the reservoir, E_F (see Fig. 36.1(a)). This makes the spin read-out very sensitive to charge switches, which can easily push the $\uparrow$ level above E_F, or pull $\downarrow$ below E_F,resulting in a measurement error. To counteract this effect, a large enough Zeeman splitting is required (in Ref. [6] a magnetic field of more than 8 Tesla was used, although with a more stable sample a lower field might be sufficient). On the

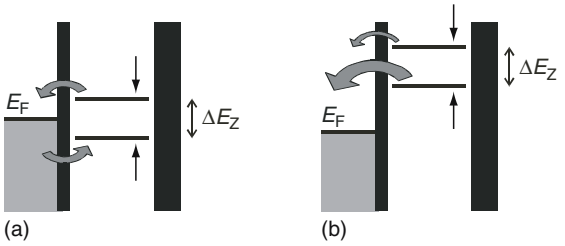

FIGURE 36.1. Schematic energy diagrams depicting (**a**) spin-to-charge conversion based on a difference in *energy* on a difference in *tunnel rate* (**b**) between $\uparrow$ and $\downarrow$.

other hand, a smaller Zeeman splitting is desirable because it implies a lower and therefore more convenient resonance frequency for coherent spin manipulation. In addition, the spin relaxation time is expected to be longer at smaller ΔE_Z. Therefore, a different spin read-out mechanism that is less sensitive to charge switches and can function at lower fields would be very useful.

A particularly convenient way to perform spin-to-charge conversion could be provided by utilizing not a difference in *energy* between spin-up and spin-down, but a difference in *tunnel rate* (Fig. 36.1(b)). To read out the spin orientation of an electron on the dot, we simply raise both dot levels above E_F, so that the electron can leave the dot. If the tunnel rate for spin-up electrons, $\Gamma_\uparrow$ is much larger than that for spin-down electrons, $\Gamma_\downarrow$, then at a suitably chosen time the dot will have a large probability to be already empty if the spin was up, but a large probability to be still occupied if the spin is down. Measuring the charge on the dot within the spin relaxation time can then reveal the spin state.

This scheme is very robust against charge switches, since no precise positioning of the dot levels with respect to the leads is required: both levels simply have to be above E_F. Also, switches have a small influence on the tunnel rates themselves, as they tend to shift the whole potential landscape up or down, which does not change the tunnel barrier for electrons in the dot.[8] Of course, the visibility of this spin measurement scheme depends on the difference in tunnel rate tha can be achieved .

A difference in tunnel rate for spin-up and spin-down electrons is provided by the magnetic field. From large-bias transport measurements in a magnetic field parallel to the 2DEG,[9] it was found that the spin-selectivity ($\Gamma_\uparrow/\Gamma_\downarrow$) grows roughly linearly from ~ 1.5 at 5 T to ~ 5 at 14 T. This is in good agreement with the spin-selectivity of about 3 that was found at 10 T using the single-shot spin measurement technique of Ref. [6].

In a magnetic field parallel to the 2DEG, the effect only leads to a modest spin-selectivity that does not allow a single-shot measurement. However, a much larger spin-selectivity is possible in a perpendicular magnetic field, i.e., in the quantum Hall regime. Magnetotransport measurements in 2DEGs with odd filling factor have shown that the effective g-factor can be enhanced by as much as a factor of ten, depending on the field strength.[10] In this case, $\downarrow$ electrons tunneling into or out of the dot experience a thicker tunnel barrier than $\uparrow$ electrons, resulting in a difference in tunnel rates.[11] A convenient perpendicular field of ~ 4 T is anticipated to give enough spin-selectivity to allow high-fidelity spin read-out.

36.3 Initialization

Initialization[6] of the spin to the pure state $\uparrow$ – the desired initial state for most quantum algorithms have been demonstrated. By waiting long enough, energy relaxation will cause the the spin on the dot to relax to the $\uparrow$ ground state (Fig. 36.2(a)). This is a very simple and robust initialization approach, which can be used for any magnetic field orientation (provided that $g\mu_B B > 5k_B T$). However, as it takes about $5T_1$ to reach equilibrium, it is also a very slow procedure (~ 10 ms), especially at lower magnetic fields, where the spin relaxation time T_1 might be very long.

A faster initialization method is to place the dot in the read-out configuration (Fig. 36.2(b)), where a spin-up electron will stay on the dot, whereas a spin-down electron will be replaced by a spin-up.[6] After waiting a few times the sum of the typical tunnel times for spin-up and spin-down ($\sim 1/\Gamma_\uparrow + 1/\Gamma_\downarrow$), the spin will be with large probability in the $\uparrow$ state. This initialization procedure can therefore be quite fast (< 1 ms), depending on the tunnel rates.

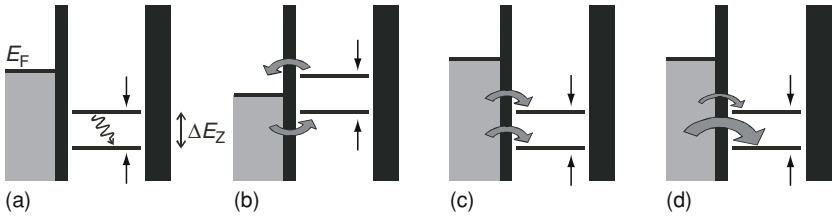

FIGURE 36.2. Schematic energy diagrams depicting initialization procedures in a large parallel or perpendicular magneticfield. (**a**) Spin relaxation to pure state ↑. (**b**) The 'read-out' configuration can result in ↑ faster. (**c**) Random spin injection gives a statistical mixture of ↑ and ↓. (**d**) In a large perpendicular field providing a strong spin-selectivity, injection results mostly in ↑.

To initialize the dot to a mixed state is also possible, where the spin is probabilistically in ↑ or ↓. In Ref. [6], mixed-state initialization was demonstrated in a parallel field by first emptying the dot, followed by placing both spin levels below E_F during the 'injection stage' (Fig.36.2(c)). The dot is then randomly filled with either a spin-up or a spin-down electron. This is very useful, e.g., to test two-spin operations.

In a large perpendicular field providing a strong spin-selectivity, initialization to the ↑ state is possible via spin relaxation (Fig.36.2(a)) or via direct injection (Fig. 36.2(d)). Initialization to a mixed state (or in fact to any state other than ↓) is very difficult due to the spin-selectivity. It probably requires the ability to coherently rotate the spin from ↑ to ↓ (see Section 36.5).

36.4 Coherence Times

The long-term potential of GaAs quantum dots as electron spin qubits clearly depends crucially on the spin coherence times T_1 and T_2. It has been shown that the single-spin relaxation time, T_1, can be very long – on the order of 1 ms at 8 T.[6] This implies that the spin is only very weakly disturbed by the environment. The dominant relaxation mechanism at large magnetic field is believed to be the coupling of the spin to phonons, mediated by the spin-orbit interaction.[12]

The fundamental quantity of interest for spin qubits is the decoherence time of a single electron spin in a quantum dot, T_2, which has never been measured. Experiments with electrons in 2DEGs have established an ensemble-averaged decoherence time, T_2^*, of ~ 100 ns.[13] A similar lower bound on T_2 has been claimed for a single trapped electron spin, based on the linewidth of the observed electron spin resonance.[14] Theoretically, it has been suggested that the real value of T_2 can be much longer,[12] and under certain circumstances could even be given by $T_2 = 2T_1$, limited by the same spin-orbit interactions that limit T_1.

36.5 Coherent Single-spin Manipulation: ESR

The key requirement for an actual spin qubit is yet to be satisfied: coherent manipulation of one- and two-spin states. To create controllable superpositions of ↑ and ↓, the well-known Electron Spin Resonance (ESR) effect can be used. A microwave magnetic field B_{ac} oscillating in the plane perpendicular to B, at a frequency $f = g\,\mu_B B/h$ (in resonance with the spin precession

about B) causes the spin to make transitions between $\uparrow$ and $\downarrow$. The choice of B strength is a trade-off between reliable initialization and read-out (strong B is better) and experimental convenience (low f is easier). It is expected that a perpendicular field of 4 T should be sufficient to provide high-fidelity read-out and initialization, with $f \approx 25$ GHz (for $g = -0.44$). Alternatively, in a parallel field we may have to go up to 8 T, corresponding to $f \approx 45$ GHz,[15] for high-fidelity spin measurement. However, since single-shot read-out is not strictly required, a somewhat lower field could also be enough.

Properly timed bursts of microwave power tip the spin state over a controlled angle, e.g., 90° or 180°. In order to observe Rabi oscillations, the Rabi period must be at most of the order of the single-spin decoherence time T_2. For a Rabi period of 150 ns, we need a microwave field strength B_{ac} of ~ 1 mT. If T_2 is much longer, there is more time to coherently rotate the spin, so a smaller oscillating field is sufficient.

We intend to generate the oscillating magnetic field by sending an alternating current through an on-chip wire running close by the dot (Fig. 36.3(a)). If the wire is placed well within one wavelength (which is a few mm at 30 GHz near the surface of a GaAs substrate) from the quantum dot, the dot is in the near-field region and the electric and magnetic field distribution produced by the AC current should be the same as for a DC current. With a wire 200 nm from the dot, a current of ~ 1 mA should generate a magnetic field of about 1 mT and no electric field at the position of the dot. To minimize reflection and radiation losses, the wire is designed to be a shorted coplanar stripline (Fig. 36.3(b)) with a 50Ω impedance.

To detect the ESR and obtain a lower bound on T_2 from the linewidth of the resonance signal, various methods have been proposed, either using transport measurements[16] or relying on charge detection.[17] In both cases, the required spin-to-charge conversion is achieved by positioning the dot levels around the Fermi energy of the reservoir (Figs. 36.4(a) and (b)). The ESR field induces spin flips, exciting $\uparrow$ electrons to $\downarrow$, which can then tunnel out of the dot. This leads to an average current (Fig. 36.4(a)) or to a change in the average occupation of the dot (Fig. 36.4(b)). However, in this configuration the dot is particularly sensitive to spurious effects induced by the microwaves, such as $\uparrow$ electrons being excited out of the dot via thermal excitation or photon-assisted tunneling. These processes can completely obscure the spin resonance.

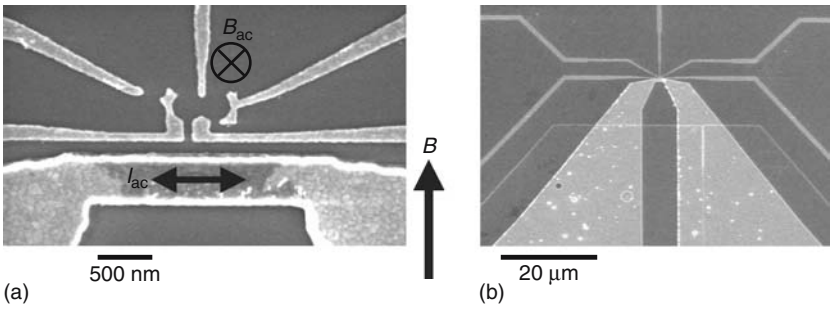

FIGURE 36.3. On-chip wire to apply microwaves to a nearby quantum dot. (**a**) Scanning electron microscope image of a device consisting of a double quantum dot in close proximity to a gold wire. An AC current through the wire, I_{ac}, generates an oscillating magnetic field, B_{ac}, perpendicular to the plane. If the AC frequency is resonant with the Zeeman splitting due to a large static in-plane magnetic field, B, a spin on the dot will rotate. (**b**) Large-scale view of the wire, designed to be a 50 Ω coplanar stripline.

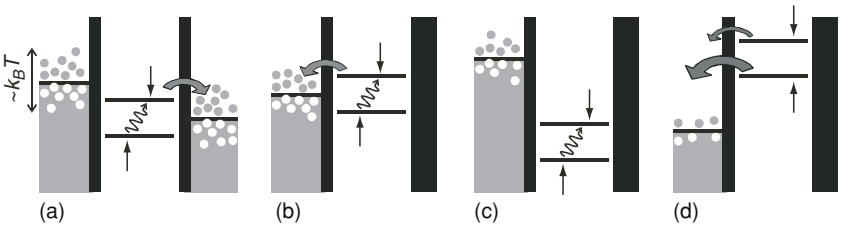

FIGURE 36.4. Detecting ESR. (**a**) To detect ESR in a transport measurement,[16] the dot is placed in Coulomb blockade, so that electron spins that are flipped by the ESR field can contribute to a current. (**b**) A similar configuration is used to detect ESR via changes in the occupation of the dot,[17] measured using a charge detector. (**c**) If the dot is deep in Coulomb blockade during the spin-flip stage, the electron is not easily excited to the reservoir via thermal excitation or photon-assisted tunneling. (**d**) The microwaves are off during the spin read-out stage to enhance the measurement fidelity.

Such problems can be avoided by combining (pulsed) electron spin resonance with *single-shot* spin measurement. This allows us to separate the spin manipulation stage (during which the microwaves are on) from the spin read-out stage (without microwaves). In this way, excitation out of the dot is prevented by Coulomb blockade (Fig. 36.4(c)), until spin read-out is initiated (Fig. 36.4(d)). In contrast to the techniques described above – which require a large spin flip rate to generate a *measurable* current or disturbance of the dot occupation – this approach only requires the spin flip rate to be faster than the decoherence rate. Therefore, a longer T_2 allows us to use a smaller B_{ac}, corresponding to (quadratically) smaller microwave power. This should help to suppress heating and photon-assisted tunneling.

In principle, an ESR experiment can be performed in a parallel or a perpendicular magnetic field. The read-out in a perpendicular field is particularly suitable for ESR detection, as the dot levels are far above E_{F} (so are not affected by photon-assisted tunneling or heating). If B is perpendicular to the surface, B_{ac} must run through the dot in a direction parallel to the surface, so the wire must be placed above the dot rather than to its side. The wire could be located on top of an insulating dielectric layer that covers the gate electrodes.

36.6 Coherent Spin Interactions: $\sqrt{\mathrm{SWAP}}$

Two electron spins S_1 and S_2 in neighboring quantum dots are coupled to each other by the exchange interaction, which takes the form $J(t) = S_1 \cdot S_2$. If the double dot is filled with two identical spins, the interaction does not change their orientation. However, if the left electron spin starts out being $\uparrow$ and the right one $\downarrow$, then the states of the two spins will be swapped after a certain time. An interaction active for half this time performs the $\sqrt{\mathrm{SWAP}}$ gate, which has been shown to be universal for quantum computation when combined with single qubit rotations.[18] In fact, the exchange interaction is even universal by itself when the state of each qubit is encoded in the state of three electron spins.[19]

The strength $J(t)$ of the exchange interaction depends on the overlap of the two electron wavefunctions, which varies exponentially with the voltage applied to the gate controlling the inter-dot tunnel barrier. By applying a (positive) voltage pulse with a certain amplitude and duration, the exchange interaction can be temporarily turned on, thereby performing a $\sqrt{\mathrm{SWAP}}$ gate.

It is expected that J may correspond to a frequency of $\sim 10\,\mathrm{GHz}$, so two-qubit gates could be performed in $\sim 100\,\mathrm{ps}$. A much larger value would not be convenient experimentally, as the exact amplitude and duration of the pulse have to be controlled very precisely. On the other hand, a very slow exchange operation would be more sensitive to decoherence resulting from fluctuations in the tunnel rate, due to charge noise. The value of J can in principle be determined in a transport measurement,[20] or alternatively by using a QPC tunneling spectroscopy technique.[4] However, in practical situations J might be too small to be resolved.

To explore the operation of the SWAP gate, reliable initialization and read-out is only needed, without requiring ESR. Imagine qubit 1 is prepared in a pure state $\uparrow$ and qubit 2 is prepared in a statistical mixture of $\uparrow$ and $\downarrow$. Measurement of qubit 1 should then always give $\uparrow$, while measurement of qubit 2 should give probabilistically $\uparrow$ or $\downarrow$. After application of the SWAP gate, in contrast, measurement of qubit 2 should always give $\uparrow$, while measurement of qubit 1 should give a probabilistic outcome. This and other spin-interaction experiments are probably easiest in a parallel magnetic field, where initialization to a statistical mixture is convenient. In addition, a large perpendicular field shrinks the electron wavefunctions, lowering the tunnel coupling and thus the exchange interaction between the two dots.

36.7 Conclusion

It has been demonstrated that single electrons trapped in GaAs lateral quantum dots are promising candidates for implementing a spin qubit. The 'hardware' for such a system is: a device consisting of two coupled quantum dots that can be filled with one electron spin each, flanked by two quantum point contacts. Using these QPCs as charge detectors, we can determine all relevant parameters of the double dot can be determined. In addition, a technique has been developed to measure the spin orientation of an *individual* electron. Now all these ingredients can be combined with the ability to generate strong microwave magnetic fields close to the dot, and gate voltage pulses to control the inter-dot coupling, in order to demonstrate superposition and entanglement of spin states.

Acknowledgments. We thank C. J. P. M. Harmans, W. G. van der Wiel, M. Blaauboer, S. Tarucha, and D. Loss for useful discussions. We acknowledge financial support from the Specially Promoted Research Grant-in-Aid for Scientific Research from the Japanese Ministry of Science; DARPA grant DAAD19-01-1-0659 of the QuIST program; the Dutch Organization for Fundamental Research on Matter (FOM); and the European Union through a TMR Program Network.

References

1. D. Loss and D. P. DiVincenzo, *Phys. Rev. A* **57**, 120 (1998).
2. D. P. DiVincenzo, *Fortschr. Phys.* **48**, 771 (2000).
3. J. M. Elzerman, R. Hanson, J. S. Greidanus, L. H. Willems van Beveren, S. De Franceschi, L. M. K. Vandersypen, S. Tarucha, and L. P. Kouwenhoven *Phys. Rev. B* **67**, 161308 (2003).
4. J. M. Elzerman, R. Hanson, L. H. Willems van Beveren, L. M. K. Vandersypen, and L. P. Kouwenhoven, *Appl. Phys. Lett.* **84**, 4617 (2004).
5. J. R. Petta, A. C. Johnson, C. M. Marcus, M. P. Hanson, and A. C. Gossard, cond-mat/0408139 (2004).

6. J. M. Elzerman, R. Hanson, L. H. Willems van Beveren, B. Witkamp, L. M. K. Vandersypen, and L. P. Kouwenhoven, *Nature* **430**, 431 (2004).
7. R. J. Schoelkopf, P. Wahlgren, A. A. Kozhevnikov, P. Delsing, and D. E. Prober, *Science* **280**, 1238 (1998).
8. S .W. Jung, T. Fujisawa, Y. H. Jeong and Y. Hirayama, *Appl. Phys. Lett.* **85**, 768 (2004).
9. R. Hanson, B. Witkamp, L. M. K. Vandersypen, L. H. Willems van Beveren, J. M. Elzerman, and L. P. Kouwenhoven, *Phys. Rev. Lett.* **91**, 196802 (2003).
10. T. Englert, D. C. Tsui, A. C. Gossard, and C. Uihlein, *Surf. Sci.* **113**, 295 (1982).
11. M. Ciorga *et al.*, *Phys. Rev. B* **61**, R16315 (2000).
12. V. N. Golovach, A. Khaetskii, and D. Loss, *Phys. Rev. Lett.* **93**, 016601 (2004).
13. J. M. Kikkawa and D. D. Awschalom, *Nature* **397**, 139 (1999).
14. M. Xiao, I. Martin, E. Yablonovitch, and H. W. Jiang, *Nature* **430**, 435 (2004).
15. R. Hanson, L. M. K. Vandersypen, L. H. Willems van Beveren, J. M. Elzerman, I. T. Vink, and L. P. Kouwenhoven, cond-mat/0311414 (2003).
16. H. A. Engel and D. Loss, *Phys. Rev. Lett.* **86**, 4648 (2001).
17. I. Martin, D. Mozyrsky, and H. W. Jiang, *Phys. Rev. Lett.* **90**, 018301 (2003).
18. G. Burkard, D. Loss, and D. P. DiVincenzo, *Phys. Rev. B* **59**, 2070 (1999).
19. D. P. DiVincenzo, D. P. Bacon, D. A. Lidar, and K. B. Whaley, *Nature* **408**, 339 (2000).
20. V. N. Golovach and D. Loss, *Phys. Rev. B* **69**, 245327 (2004).